INORGANIC CHEMISTRY

FRONTIERS

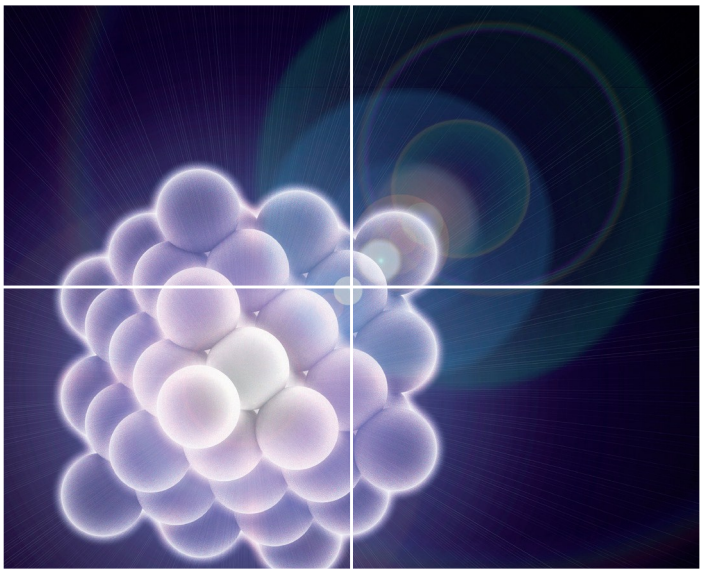

Accepted Manuscript

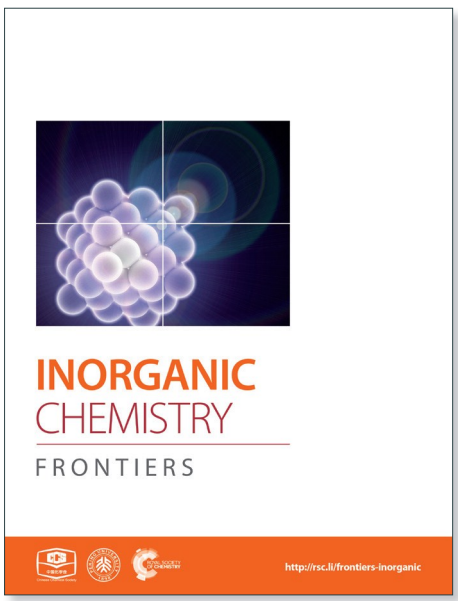

This is an *Accepted Manuscript*, which has been through the Royal Society of Chemistry peer review process and has been accepted for publication.

Accepted Manuscripts are published online shortly after acceptance, before technical editing, formatting and proof reading. Using this free service, authors can make their results available to the community, in citable form, before we publish the edited article. We will replace this *Accepted Manuscript* with the edited and formatted *Advance Article* as soon as it is available.

You can find more information about *Accepted Manuscripts* in the **Information for Authors**.

Please note that technical editing may introduce minor changes to the text and/or graphics, which may alter content. The journal's standard **Terms & Conditions** and the **Ethical guidelines** still apply. In no event shall the Royal Society of Chemistry be held responsible for any errors or omissions in this *Accepted Manuscript* or any consequences arising from the use of any information it contains.

A Review of Metal Oxynitrides for Photocatalysis

Manan Ahmed* and Guo Xinxin

Department of Environmental Engineering, Faculty of Engineering and Green Technology, Universiti Tunku Abdul Rahman, Perak, Malaysia

**Email: manan_ahmed@live.com*

Abstract: Photocatalytic hydrogen (H_2) production represents a very promising but challenging contribution to a clean, sustainable and renewable energy system. Photocatalytic water splitting into hydrogen and oxygen is a method to directly convert solar energy into storable chemical energy, and has received considerable attention for use in large scale solar energy utilization because of its great potential for low cost and clean energy production. Developing efficient and cost-effective photocatalysts for water splitting is a growing need, and semiconductor photocatalysts have recently attracted more attention due to their stability and simplicity. Over the past few decades, various metal oxides photocatalysts for water splitting have been developed and their photocatalysis application studied under UV irradiation. To harness solar energy efficiently, a recent main concern has been the development of visible-light ($\lambda > 400$ nm) active photocatalysts for water splitting. Metal oxynitride are emerging materials that may combine the properties of oxides and nitride. Metal Oxynitrides photocatalyst are of significant interest in the field of photocatalysis in water splitting as the observed small band gaps lead to activity in the visible range. Titanium, tantalum, niobium, gallium and zirconium form important photocatalysts which show promise in visible light-driven photoreactions. Along with perovskite structures, development of double complex perovskites oxynitride that are active under visible light is also reviewed.

This review article provides a board overview of the development of water-splitting photocatalysts for generating hydrogen, summarizing the current state of work with a focus on recent progress in visible-light induced overall water splitting on oxynitrides photocatalysts.

Keywords: Oxynitrides, Photocatalysis, Solar energy.

1. INTRODUCTION

Providing clean and renewable energy is arguably the most important challenge facing humanity in the 21st century. The world's energy demand is projected to more than double by mid-century and more than triple by 2100 [1]. One of the most important goals of our modern

society is to construct a sustainable environment. Growing environmental concerns related to the extensive use of non-sustainable fossil fuels (oil, natural gas and coal) and a constantly increasing energy demand will force mankind, sooner or later, to tap into clean and sustainable sources of energy.

Capturing solar energy by splitting water into hydrogen and oxygen long been considered a favorable idea, in 1874 Jules Verne, recognizing the predictable source of coal and potentials of hydrogen derived from water electrolysis, made the comment that "water will be the coal of the future" [2]. Water electrolysis by means of solar light mimics photosynthesis by converting water into H_2 and O_2 using inorganic photo-semiconductors (photocatalyst) that catalyzed the water-splitting reaction. Hydrogen is a clean energy carrier because the chemical energy stored in the H-H bond easily released when it combines with oxygen, yielding only water vapor's as the reaction by-product. Hydrogen (H_2) is widely considered to be the future clean energy carrier in many applications, such as environmentally friendly vehicles, domestic heating, and stationary power generation. Currently, large-scale hydrogen production is performed by reforming or gasifying fossil fuels [3].

Photocatalysis has long been studied and is expected to make a great contribution to both environmental treatment (emission cleaning and water purification) and renewable energy. Over the past few decades, the number of application based on photocatalysis increased sharply; while a wide range of material systems have been developed [4]. Photocatalytic H_2 production from water is one of the most promising ways to realize a hydrogen economy for three reasons. (1) This technology is based on photon (or solar) energy, which is a clean, permanent source of energy, and mainly water, which is a renewable resource; (2) it is an environmentally safe technology without undesirable by-products and pollutants; and (3) the photochemical conversion of solar energy into a storable form of energy, i.e. hydrogen allows to deal with the intermittent character and seasonal variation of the solar influx.

Essential prerequisite for the photocatalyst is its resistance to reaction at solid/liquid interface, which can comprise its properties. However, it has proven difficult to find an ideal photocatalyst, which meets all the requirements (chemical stability, corrosion resistance, visible light harvesting and suitable band edges) that would render photocatalytic H_2 production a viable alternative. Fortunately, Nano science and nanotechnology have boosted the modification of existing photocatalysts and the discovery and development of new candidate materials [5]. The

rapidly increasing number of scientific publications constitutes clear bibliographical evidence for the significance of this hot topic. Since 2004, the number of publications on nano photocatalytic H_2 production has increased by a factor of about 1.5 times every year. Many papers studied the impact of different nanostructures and nanomaterials on the performance of photocatalysts, since their energy conversion efficiency is principally determined by nano-scale properties.

Transition-metal nitrides and oxynitrides are an important class of emerging materials that, in optimal cases, may combine the advantages of oxides and nitrides. Transition-metal oxynitrides are well suited for catalysis applications as they have good electrical conductivities and corrosion resistance. Their activities in hydro-denitrogenation and hydro-desulfurization resemble those of noble metals [6]. Generally, oxynitrides stabilities in air and moisture are greater than those of the pure nitrides, but with smaller band gaps than those of comparable oxides. This leads to useful electronic and/or optical properties, such as the N-doping of TiO_2 to tune the band gap from the ultraviolet to the visible region for photocatalysis. Many useful oxynitrides of high valence (d^0 electron configuration) transition metals adopt the AMX_3 (X=N/O) perovskite-type crystal structure; $CaTaO_2N$ and $LaTaON_2$ solid solutions are non-toxic, red-yellow pigments, $BaTaO_2N$ has a high dielectric constant and photocatalysis the decomposition of water and $EuNbO_2N$ and $EuWON_2$ are ferromagnetic and show colossal magneto resistances [7].

We choose oxynitride for major chemical space to implement the photocatalysis in this review because most of the existing photocatalysts are oxides [8]. However, the band gap energies of metal oxides (> 3 eV) are usually too large to absorb visible light and most of the material is active under UV light irradiation. This is mainly due to a too low valance band (VB) energy which is derived from the 2p orbitals of the oxygen atoms [9]. Therefore, photocatalyst that function in the visible light region (λ= 400–800nm) must be developed for the particle use for photocatalytic water splitting. A requirement for the visible light-induced photocatalyst is optimum band-gap energy should be less than 3 eV [10]. To solve this problem, non-oxides such as nitrides and sulfides have been proposed, since their valance band (VB) position is usually higher in energy. Unfortunately, nitrides usually suffer from poor aqueous stability and cannot maintain photocatalytic activity in water over a long period of time [11]. By changing the N/O ratio for a constant cationic composition it is possible to modulate the oxidation state of the cations modifying the physical properties. When introducing nitrogen into an oxidic network the physical and chemical properties may change even if this takes place at a doping level. Nitrogen

is less electronegative than oxygen so the optical gap between the anion-based valence band and the cation-based conduction band decreases as oxide is substituted by nitride. Nitrogen is more polarizable than oxygen, the metal-ligand bond is more covalent and this increases the nephelauxetic effect (expansion of the electron cloud), then decreasing inters electronic repulsion and the energy of the d orbitals [12]. Indeed, band gap values published for oxynitrides fall into the interval of 1.6-3.3 eV. The band gap overlap with the solar spectrum makes this class of materials interesting for applications as visible-light driven photocatalysts [13].

The review presents the progress in the study of photocatalysts for overall water splitting, with a focus on recent advances in visible-light water splitting on metal oxynitride photocatalysts.

2. MECHANISM OF PHOTOCATALYTIC WATER SPLITTING OR HYDROGEN PRODUCTION

Photocatalysis water splitting is not a catalytic process according to the traditional definition of catalysis because it is an uphill reaction. It can also be called photo-induced water splitting on a semiconductor. Photocatalytic water splitting involves a sequence of multiple competing steps, including light harvesting, charge generation, separation, transportation, recombination and surface reaction [14]. Generally, inorganic-based semiconductors are used for photocatalysis and their electronic structure plays key role in photocatalysis water splitting. An ideal semiconductor/ photocatalyst should have a band gap, E_g that constitutes the energy difference between the conduction band (CB) and the valence band (VB) with sufficient energy to drive the water splitting reaction. Solid materials have an electronic structure with some empty and some filled electronic states. If there is an energy gap between these two sets of electronic states, the material is classified as a semiconductor or insulator. The filled and empty energy states called valance and conduction band, the energy gap between valance and conduction band called the band gap.

The basic working principle of photocatalysis is simple and similar to electrolysis. In the ground state, all electrons exist in the valance band (VB) and under visible light irradiation the semiconductor (photocatalyst) absorbs a photon to excite an electron from the valence band to the conduction band: resulting in an excited state and the formation of an electron (e^-)-hole (h^+) pair. The lifetime of an e^--h^+ pair is only a few nanoseconds, but this may be enough to promote redox reaction. The photo-generated electrons and holes cause redox reactions similarly to

electrolysis. These photo-generated electrons and hole may recombine in the bulk or on the surface of photocatalyst. The two protons, which are required to generate hydrogen gas, can use the electrons that are excited in the photocatalyst. The hole in the valence band can be filled with an electron produced by the oxygen generation (Fig. 1)[15].

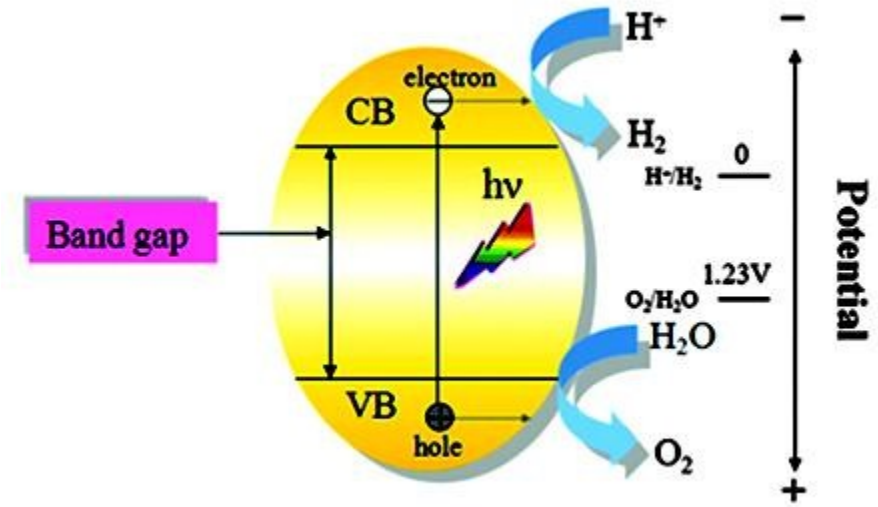

Figure 1: Mechanism of photocatalytic water splitting (reproduced from the ref. 15 with permission from the Royal Society of Chemistry).

One requirement for photocatalytic water splitting is that the conduction band (CB) and valence band (VB) for a semiconductor material should straddle the redox potentials for H^+/H_2 and H_2O/O_2. For H_2 production to occur, the conduction band-edge must be more negative than the reduction potential of H^+ to H_2 (E_{H^+}/H_2 =0 V vs NHE at pH=0), while the valance band top-edge should be more positive than the oxidation potential of H_2O to O_2 ($E_{O2/H2O}$= 1.23 vs NHE at pH=0) for O_2 formation from water to occur [16]. Thermodynamically, the theoretical minimum photon energy required splitting water into hydrogen and oxygen corresponding to a 2-electron transfer step is 1.23 eV. This photon energy 1.23 eV is equivalent to a 1000 nm wavelength and it is located in near infrared region. However, Murphy et al. determined that there are fundamental thermodynamic limits to the photo conversion efficiency, which depend on the band-gap of the semiconductor being used, and on the spectrum of the incident radiation. These limiting efficiencies cannot be achieved, due to losses such as the incomplete absorption of the incident radiation in the semiconductor, reflection of the incident radiation from the surface of the semiconductor and other surfaces. The actual minimum required band gap for the photocatalytic overall water splitting is estimated to be approximately 2 eV [17]. So that the visible

light (400-800 nm in wavelength) that represents half of the solar energy spectrum can be thermodynamically used for water splitting. The challenge is to obtain an efficient photocatalyst that has an absorption edge in longer wavelength and the ability to split water [18]. However, in practice, a slightly higher photon energy is necessary due to the presence of over potentials, and a photon energy of 1.7 eV (730 nm) is thought to be a realistic goal.

3. METHOD OF SYNTHESES OF OXYNITRIDES

The syntheses of nitride-based materials are less straight forward than for oxides because of their lower stability. To synthesize oxynitrides from oxides a suitable nitriding agent is required. The most common method for the syntheses of ternary oxynitrides is the thermal treatment at high temperature (between 1300°C and 1600°C) containing stoichiometric mixture of metal oxides, carbonates and/or nitrides under a high-pressure $N_{2(g)}$, or a mixture N_2/H_2 (typically 90/10 or 95/5 % v/v) if reducing conditions are required [19]. The use of high pressure is expected to be a general and very convenient approach in oxynitrides synthesis since it suppresses the decomposition to oxides and nitrogen gas and it should be useful for the stabilization of new phases at moderate temperatures. High pressure is also expected to stabilize oxynitrides structure with high coordination numbers for cations and anions as for instance perovskite [12]. However, very few direct solid-state syntheses of oxynitrides at high pressures have been reported.

Ammonolysis of a precursor oxide has been well documented as simple experimental technique and inexpensive method for the syntheses of a wide variety of oxynitride products. Ammonolysis of oxides under flowing NH_3 gas has enabled many new oxynitrides to be synthesized in which ammonia behaves as a nitriding agent and additionally induces a change in the oxidation state of the involved transition metals. Due to the high bonding energy of the N to N triple bond, the application of N_2 in syntheses usually requires high activation energy [20]. The corresponding reaction between a suitable solid precursor and gaseous ammonia is often referred to as “thermal ammonolysis”.

Due to the large difference in the free energies of formation between the binary rare earth oxides and nitrides, the ammonolytic syntheses of rare earth quaternary oxynitrides usually start with ternary oxides ($A_2B_2O_7$, ABO_4 with a B-site cation being in its stable oxidation state) or oxides-carbonates mixtures (ACO_3–B_xO_y), are most often used precursors for the perovskite-type oxynitrides synthesis [21, 22]. Nitridation reaction are usually carried out in an alumina boat

comprising the oxide precursor powder place inside an alumina tube through which ammonia gas flows normally at a rate up to 30-40 L/h at 800 °C. The reaction between a precursor and ammonia is usually carried out at atmospheric pressure in the temperature region of T = 600-1000 °C, depending on the precursor and system used, with a heating rate of about 10 °C/min. The ammonia flow rate depends on the reaction temperature; higher the temperature, higher the rate in order to minimize the dissociation of NH_3 into dinitrogen and dihydrogen before reaching the product [22]. The key parameters for the ammonolysis reaction are temperature, nitrogen flow rate; reaction time and sample placement in the reaction tube and gas composition (NH_3, N_2 and H_2) around the sample should be considered to optimize the purity of the oxynitride phase [23]. Ammonia acts as a reducing and an oxidizing (nitriding) agent, this dual behavior nitriding and reducing is essential for the ammonolysis reaction.

Ammonia decomposition reactions on oxides surfaces are not well studied. However, it is suggested that ammonia dissociates at the surface, forming active nitriding species (N, NH, NH_2) in a native state and molecular hydrogen [24]. The highly reactive hydrogen combines with oxygen atoms from the oxides and eliminates them as a water vapor; the formation of water vapors provides the thermodynamic driving force in the reaction, while nitrogen is introduced into the lattice through substitution. Several types of metallic compounds can be nitride with the help of flowing ammonia gas by using adequate temperatures. At a sufficiently high temperature range 450-1200℃, the use of ammonia gas at atmospheric pressure is equivalent to using $N_{2\,(g)}/H_{2\,(g)}$ at high pressure [25].

$$\text{Oxide} + NH_{3\,(g)} \longrightarrow \text{Oxynitride} + H_2O_{(v)}\uparrow$$

Thin films of functional oxynitrides have been synthesized using physical and chemical methods. Pulsed laser deposition (PLD) was employed for the synthesis of thin films of perovskites with dielectrical properties as $BaTaO_2N$ [26] and reactive radio frequency magnetron sputtering has been used for the preparation of thin films of $LaTiO_2N$ with photo-catalytical applications [27]. Nanostructured meso-porous nitrogen doped TiO_2 films have been prepared by combining of sol–gel, templating and ultrafast evaporation-induce self-assembly followed by controlled treatment in NH_3 gas [28].

4. OXYNITRIDES PHOTOCATALYST FOR VISIBLE LIGHT UTILIZATION

Research in this field of photocatalysis was initiated by the pioneering work conducted Honda and Fujishima in 1972 [29]. Since the discovery of the Honda-Fujishima effect, numbers of

experiments have been conducted to establish new stable photocatalytic powder systems which were mostly based on metal oxides and oxynitrides to stiochiometrically split water into H_2 and O_2 [30]. Many types of semiconductors over the past 40 years, with over 130 materials including oxides, nitrides, sulfides, carbides, and phosphides, have been reported to act as efficient particle photocatalysts for hydrogen evolution via water splitting. Unfortunately, most of the photocatalysts are active only under UV light, and materials active under visible light are quite limited. More recently non-oxide materials such as sulfides, oxynitrides and oxysulfides have been found to be active for H_2 and O_2 evaluation under visible light irradiation (Table 1). So far, the quantum efficiency for overall water splitting over visible light driven particle photocatalysts only achieves low values and still the current 'bottleneck' of the hydrogen production from solar light.

Solar spectrum comprises 4-5 % of ultraviolet light whereas approximately 40% of solar photons are in visible region. Most of the reported photocatalyst are metal oxide. A major drawback of pure metal oxide is the large band gap restrict the utilization of visible light which are the main component of the solar spectrum and it can only be activated upon irradiation of UV light ($\lambda \leq 387$ nm for anatase), limiting the practical efficiency of solar application [31]. Therefore a current research focus is to develop a stable visible light responsive photocatalyst capable of achieving overall water splitting. Only handful of bulk oxynitrides materials of d^0 and d^{10} electronic configuration transition metal cations are the primary usable metal components for a water splitting photocatalyst under visible light because their orbitals can form a suitable conduction band. The valence bands of these oxynitride materials are populated by hybridized N_{2p} and O_{2p} orbitals while the conduction is mostly composed of the empty d orbitals of corresponding metal ions, resulting in more negative valence band levels and smaller band gaps compared to those of conventional oxide semiconductors, allowing visible-light induced H_2 production from water [16, 32-34]. In this case, it is expected that the conduction band levels are not significantly affected because the cationic components are not changed [35]. Since N^{3-} has a similar ionic radius to that of O^{2-} partial or full substitution of N^{3-} for all or part of the O^{2-} in the oxide is possible in some cases.

The photocatalysts material for water splitting are usually in the form of particles or powders suspended in aqueous solution in which each particle acts as a micro-photoelectrochemical cell that performs both the oxidation and the reduction reactions of water on its surface.

Table 1: Overview of Photocatalysts developed in past several years under visible light photocatalysis

Photocatalysts	
Titanium oxide and titanates Oxide	*Metal Oxynitrides*
TiO_2-Cr-Sb	**TaON**
TiO_2-N	**$Ti_3O_3N_2$**
$SrTiO_3$-Cr-Ta	**$Zr_3O_3N_2$**
$SrTiO_3$-Cr-Sb	*Metal sulfides*
$La_2Ti_2O_7$-Cr	**CdS**
$La_2Ti_2O_7$-Fe	**CdS-CdO-ZnO**
Other transition metal oxides	**CdS-Zn**
$BiVO_4$	**ZnS-Cu**
Ag_3VO_4	**ZnS-Ni**
$SnNb_2O_6$	**ZnS-Pb**
Nb_2O_5	**$(AgIn)_xZn_{2(1-x)}S_2$**
Ta_2O_5	**$Sm_2Ti_2S_2O_5$**
$BiTaO_4$	**$(CuIn)_xZn_{2(1-x)}S_2$**
ZnO	**$(CuAg\ In)_xZn_{2(1-x)}S_2$**
Bi_2O_3	**$Na_{14}In_{17}Cu_3S_{35}$**
WO_3	*Metal Perovskite Oxynitride*
Ga_2O_3	**$LaTaON_2$**
Mixed Metal oxynitrides	**$LaMg_xTa_{1-x}O_{1+3x}N_{2-3x}$**
$(Ga_{1-x}Zn_x)(N_{1-x}O_x)$	**$CaTaO_2N$**
$(Zn_{1+x}Ge)(N_2O_x)$	**$SrTaO_2N$**
Metal Nitride	**$BaTaO_2N$**
Ta_3N_5	**$Sr_2Nb_2O_{7-x}N_x$**
Metal free Nitride	**$LaTiO_2N$**
C_3N_4	**$CaNbO_2N$**
	$SrNbO_2N$

$BaNbO_2N$

$Y_2Ta_2O_5N_2$

This eliminates the need for a conducting substrate, enabling the use of conventional synthesis routes, which are therefore much simpler and less expensive to develop and use photo electrochemical cells. However, particulate photocatalytic systems have disadvantages when compared to photo electrochemical cells with regard to the separation of charge carriers, which is not as efficient as with a photoelectrode system, and there are difficulties associated with the effective separation of the stoichiometric mixture of oxygen and hydrogen to avoid the backward reaction [3].

4.1. Tantalum Oxynitrides

Numerous typical metal oxides with d^{10}-electronic configurations have been demonstrated to be usable as photocatalysts for efficient overall water splitting. Metal oxide photocatalysts have attracted extensive research for the purposes of solar energy conversion and environmental remediation. Overall water splitting using a photocatalyst is an attractive solution for the supply of clean and recyclable hydrogen energy. Although a large number of photocatalysts have been proposed to date, most function only in the ultraviolet (wavelength < 400 nm) region (e.g., TiO2) due to the inherently large band gap of metal oxides [36]. Metal oxynitrides are candidates for visible-light responsive photocatalysts, and promising results have been reported for TaON which have suitable conduction and valence band positions to produce hydrogen and oxygen from water. It contains nitrogen that forms the tops of the valence band, and it makes its band gap energy smaller than those of metal oxides. As a result, it absorbs visible light more effectively and has better photocatalytic ability. Domen et al. demonstrated that TaON absorbed the visible light up to ca. 530 nm, with the valence band at 2.23 eV versus NHE, and exhibited a high quantum efficiency of 34% for the water photo oxidation (oxygen photo evolution) in the presence of a sacrificial oxidizing reagent such as Ag^+ [37]. They also reported that tantalum nitride (Ta_3N_5) exhibited the high photocatalytic activity for the water photo-oxidation as well, though its valence band was mainly composed of N_{2p} orbitals and located at 1.6 V versus NHE [38, 39].

Tantalum oxynitride is one of the most attractive materials not only for the half reaction, which generates hydrogen or oxygen molecules from 2 water, but also for the full reaction, which generates simultaneously hydrogen and oxygen molecules from water in the same reactor [40]. Its crystal structure is usually monoclinic, isostructural to baddeleyite ZrO_2 (β-TaON), but there is also monoclinic VO_2 (B) (γ-TaON) that is metastable consisting of sharing edge octahedral of tantalum in layers that are connected through the $Ta(ON)_6$ octahedra corners [41] and from neutron diffraction studies; oxygen and nitrogen are ordered in the two anion sites of the baddeleyite structure. However, Tantalum is hepta-coordinated and there are two crystallographically independent sites for anions where N and O order [42] (Fig. 2).

From the band structure of β-TaON, as calculated by density functional theory (DFT), the bottom of the conduction band is based on empty Ta_{5d} orbitals similar to Ta_2O_5, whereas the top of the valence band consists of a hybridization of N_{2p} and O_{2p} orbitals in which the N_{2p} contribution is larger than that of O_{2p} [43]. The potential energy of the hybridized orbital is higher than that of an O_{2p} orbital in an oxide, resulting in smaller band gap energy sufficient to absorb visible light (Fig. 3). However, problems will arise on the stability and efficiency of TaON photocatalyst because it is expected that metal-N bond in N-doped metal oxynitride are weak compared with metal-O bond in metal oxides and that photogentrated holes are trapped at higher N_{2p} induced levels at the surface, resulting in a large decrease in the oxidation power compared with the O_{2p} valance band holes. In addition, the N-doping will introduce more or less distortion in metal oxide crystal structure leading to their destabilization.

This problem studied by Nakamura et al. and reported the mechanism of water photooxidation at the surface of TaON photocatalysis using Fe^{3+} and clarify the how water photoxidation proceeds at the metal oxynitride surface. Their experiments have indicated that the TaON surface is oxidized under visible-light irradiation, indicating that the oxygen photo-evolution on TaON actually occurs on a thin Ta-oxide over-layer [44].

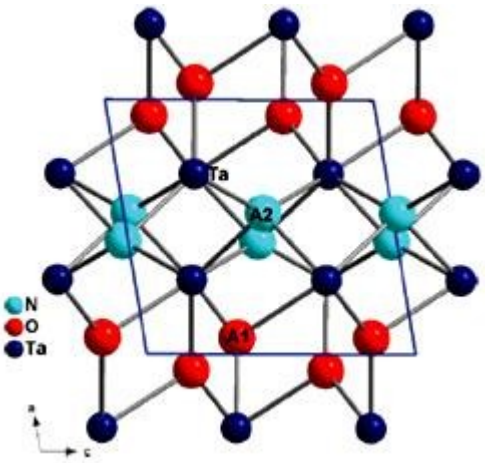

Figure 2: Crystal structure of TaON showing the coordination of two available anion sites occupied respectively by O and N (reproduced from the ref. 12 with the permission from Royal Society of chemistry).

The synthesis of β-TaON is usually done by ammonolysis of commercial Ta_2O_5 powder at 800–850 °C, using either low flow rates of NH_3 (typically 20–50 cm^3 min^{-1}) or some PH_2O (bubbling NH_3 in water) to prevent the formation of more stable phase, the nitride Ta_3N_5. As the nitridation reaction precedes the O^{2-} anions in the precursor Ta_2O_5 are gradually replaced by N^{3-} anions from the NH_3. It can also be prepared by treating Ta_2O_5 under nitrogen gas saturated with NH_4OH. Nanoparticles of β-TaON are prepared by a Ca-assisted urea route and efficient photo-anodes have been prepared by electrophoretic deposition [45].

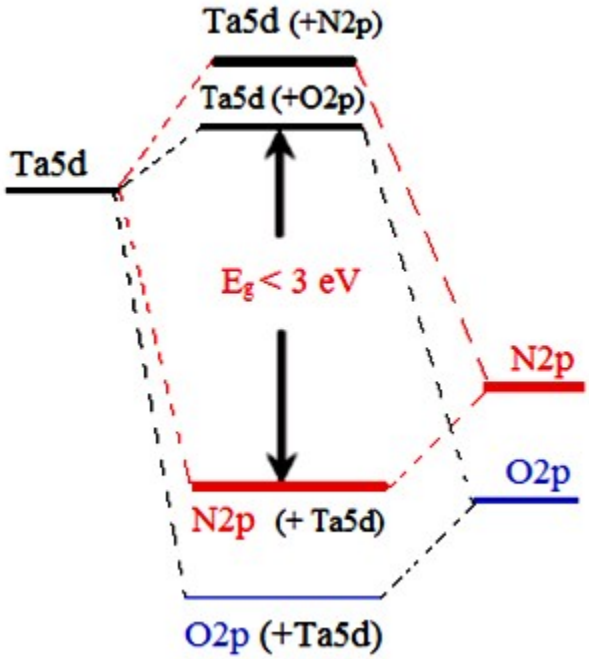

Figure 3: Schematic band structure of Tantalum oxynitride (reproduced from the ref. 46 Open Access).

4.2. Gallium-Zinc Oxynitride:

The most active photocatalyst under visible light irradiation is Gallium-zinc oxynitrides solid solution of GaN and ZnO also known as $(Ga_{1-x}Zn_x)(N_{1-x}O_x)$, one of the material that meets all the previously state condition with highest photocatalytic activity for over all water splitting [32]. This photocatalyst has an absorption edge at ~500 nm and a quantum yield of 5.2 % for 410 nm light, as shown in Fig. 4. The figure shows that absorption edges of $(Ga_{1-x}Zn_x)(N_{1-x}O_x)$ are

located at longer wavelengths than those of GaN or ZnO, but wavelengths shift to shorter with increasing nitridation. The band gap energy of the $(Ga_{1-x}Zn_x)(N_{1-x}O_x)$ is roughly estimated to be 2.6-2.8 eV based on the onsets of the diffuse reflectance spectra, which is substantially smaller than that for either GaN (3.4 eV) or ZnO (3.2 eV).

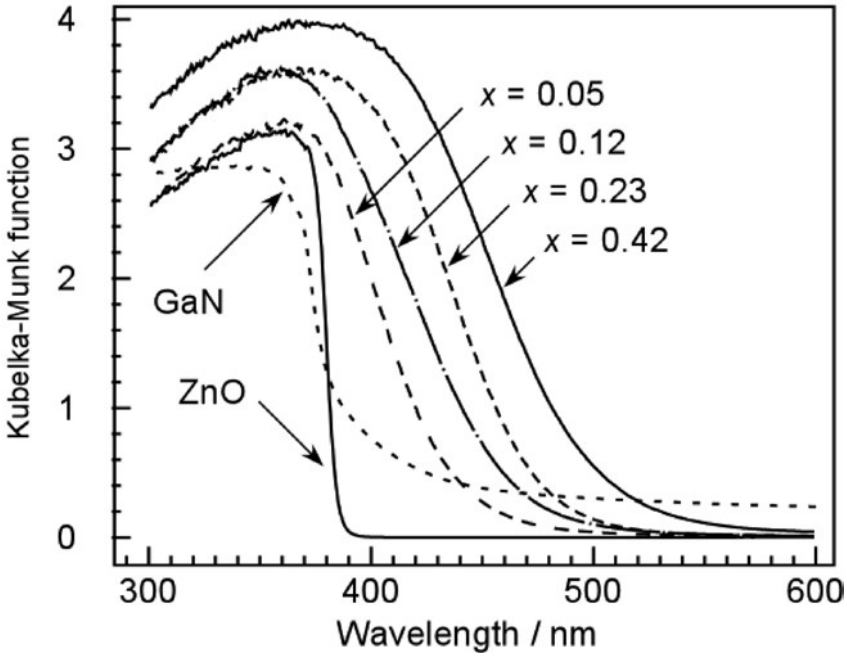

Figure 4: Diffuse reflection UV-visible spectra of $(Ga_{1-x}Zn_x)(N_{1-x}O_x)$ with varying x= 6-8. GaN and ZnO have absorption edges in the UV region (<400 nm), but the solid solution has absorption in the visible region (reproduced from ref. 32 Open Access).

GaN is a well-known material with a bandgap of 3.4 eV and has been studied extensively for application in light-emitting diodes and laser diodes [47]. GaN has also been examined as a photoelectrode, and it has been confirmed to have the potential for overall water splitting under UV irradiation [48]. The bandgap of ZnO is 3.2-3.4 eV, and it has been studied for many applications such as in light-emitting diodes and gas sensors [49, 50]. GaN and ZnO are well known material with the wurtzite crystal structures with almost the same lattice parameters and band gaps of ca. 3.4 and 3.2 eV, respectively, providing response only in the UV region (Fig. 5). However, the solid solution of the oxide and nitride, $(Ga_{1-x}Zn_x)(N_{1-x}O_x)$ with d^{10} electronic configuration, which retains the wurtzite structure, exhibits a band gap of 2.6-2.8 eV, suitable for response in the visible region. DFT calculation indicates that the small band gap is attributed to repulsion of N_{2p}-Zn_{3d} (p-d) electrons in the upper valance band, thus defining the valance band

maximum of $(Ga_{1-x}Zn_x)$ $(N_{1-x}O_x)$ [51]. Therefore, the visible light response of the solid solution originates from the contribution of Zn_{3d} atomic orbital to the valance band formation, where the bonding between Zn and N atoms is formed as a result of the formation of the solid solution.

The photocatalytic activity of $(Ga_{1-x}Zn_x)(N_{1-x}O_x)$ for water splitting under visible light (at wavelengths longer than 400 nm) is greatly enhanced by loading the catalyst surface with nanoparticles of a mixed oxide of rhodium and chromium [52]. Typically, nanoparticles of co-catalysts deposited on the surface of photocatalysts, as the hydrogen production sites, are used to enhance the rate of water reduction half-reaction. The main role of co-catalysts is to give away the photo excited electrons from the bulk of the photocatalyst and bring them to the water-photocatalyst interface. Noble metals or transition-metal oxides (e.g., Cr, Pt or Rh) are often used as co-catalysts to facilitate the water reduction half-reaction. Such co-catalysts are typically applied as nanoparticles to the photocatalyst surface by different methods including in situ photo deposition. In situ photo deposition allows the co-catalysts to be located selectively at reaction sites without the need for an activation treatment [53]. The rate of hydrogen evolution under visible light irradiation ($\lambda > 400$ nm) for GaN:ZnO solid solution was initially reported to be about 180 μmol/hg using RuO_2 as co-catalyst [54].

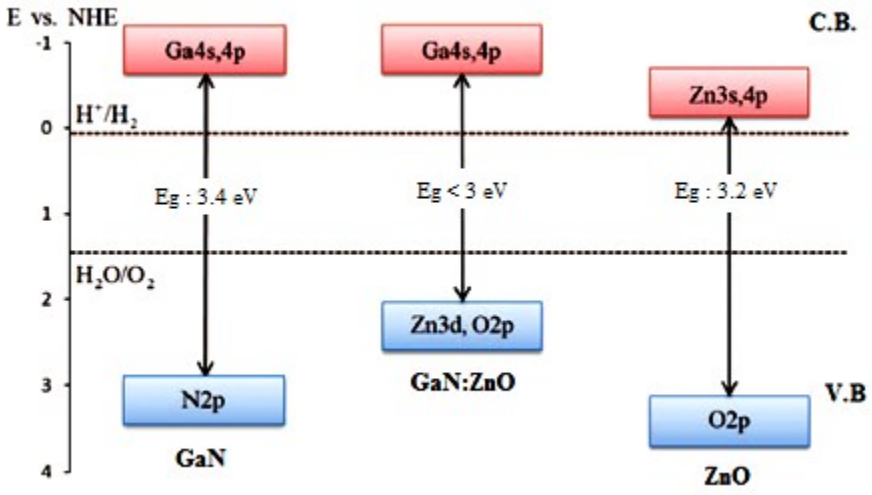

Figure 5: Schematic illustration of band structure of GaN, ZnO and GaN: ZnO solid solution (reproduced from ref. 55 with permission from Royal Society of Chemistry).

The GaN:ZnO solid solution photocatalyst is typically synthesized by nitridation of a mixture of Ga_2O_3 and ZnO (Zn: Ga= 1:1) under dry ammonia flow at high temperatures around 1223 k for 5–15 hours via the solid-state reaction process, which is the traditional method [56].

Elemental analyses by inductively coupled plasma optical emission spectroscopy (ICP-OES) have revealed that the ratios of Ga to N and Zn to O in the as-prepared material are close to unity and that the N and O concentrations increase with the Ga and Zn concentrations, respectively [57].

$$Ga_2O_3 + ZnO \xrightarrow{NH_3} (Ga_{1-x}Zn_x)(N_{1-x}O_x)$$

Although the photocatalyst prepared through the solid state reaction process demonstrates the highest activity for overall water splitting, long synthesis time and high temperatures is considered a drawback of this synthesis technique. The produces materials have relatively low surface area, bulk defects and low Zn content (usually with Zn/ (Zn+Ga) ratios of less than 15%). This composition range is far from the optimum needed to minimize the band gap. Moreover, the Zn/Ga ratio of the solid solution is very low, even with low synthesis times (<0.28 at 5 h) due to the volatilization of ZnO at high synthesis temperatures [56]. Various attempts have been made to increase the Zn content without losing the crystallinity of the synthesized photocatalyst, including the application of different precursors in different amounts, different annealing times, as well as pre- and post-treatment techniques.

Madea et al., were examined in detail the photocatalytic activities for water splitting on GaN:ZnO solid solutions for various compositions and with various loading amounts of RuO_2 cocatalyst. Among these, $(Ga_{1-x}Zn_x)(N_{1-x}O_x)$ with x = 0.12 loaded with a 5 wt. % RuO_2 showed the highest activity. H_2 and O_2 evolved steadily and stoichiometrically upon light irradiation, and the reaction continued even under visible light irradiation. The optical absorption edge and band gap for the solid solution with this composition were 482 nm and 2.68 eV, respectively. This was the first reproducible example of visible-light induced overall water splitting on a single photocatalyst system [55]. It is proposed that modification of $(Ga_{1-x}Zn_x)(N_{1-x}O_x)$ with Rh and Cr mix-oxide nanoparticles increased the quantum efficiency for overall water splitting to 2-3% at 420-440 nm, which is approximately 10 times greater than that achieved using the RuO_2- loaded catalyst. The function of the Rh-Cr-O mixed oxide nanoparticles is to trap the excited electron and holes to harness them for the photocatalytic splitting of water. The Rh^{3+} are the H_2 evolution sites and Cr^{3+} oxides shell prevent the O_2/H_2 back reaction to from water and the bulk GaZnOx or their contact points are the possible O_2 evolutions sites. Interestingly, modification of $(Ga_{1-x}Zn_x)(N_{1-x}O_x)$ with either RhO_2 or Cr oxide alone did not provide a significant increase in photocatalytic activity [57, 58].

4.3. Gallium-Zinc-Indium Oxynitrides:

A solid solution of $(Ga_{1-x}Zn_x)(N_{1-x}O_x)$, with the d^{10} electronic configuration has been reported to act as a photocatalyst for overall water splitting under visible light irradiation [32]. It has been shown that absorption edge of $(Ga_{1-x}Zn_x)(N_{1-x}O_x)$ depend on the zinc and oxygen concentration and the highest photocatalytic activity is obtained in a narrow compositional range near x = 0.18. The absorption edge band for this composition occurs at around ~500 nm. For efficient use of solar energy, compounds exhibiting an absorption band at longer wavelengths are crucial [9, 59].

Kamata et al. reported the new photocatalytic material Ga-Zn-In-O-N mixed oxynitride with d^{10} electronic configuration and a wide absorption band at visible wavelengths. One of the approaches to prepare new material to extend the absorption edge of $(Ga_{1-x}Zn_x)(N_{1-x}O_x)$ by forming a solid solution with indium nitride (InN), have the same wurtzite structure as $(Ga_{1-x}Zn_x)(N_{1-x}O_x)$. Ga-Zn-In-O-N mixed metal oxynitride have a more suitable characteristic as InN have a narrow band gap (<1 eV) as compare to $(Ga_{1-x}Zn_x)(N_{1-x}O_x)$ (2.6-2.8 eV). It exhibits an absorption band near 600 nm and demonstrates a potential for overall water splitting under visible light irradiation [60].

4.4. Titanium and Zirconium Oxynitrides:

Wu et al. reported the theoretical aspect of the two new $Ti_3O_3N_2$ and $Zr_3O_3N_2$ photocatalyst. Both of these oxynitrides material not yet reported and predicted for future work. Both of these compounds can be generate from the crystal structure of Ta_3N_5 and their crystal structures are shown in Fig. 6. The instability energy for $Ti_3O_3N_2$ is ΔH 31.0 meV/atom and 1.0 meV/atom for $Zr_3O_3N_2$. This suggests that both materials are expected to be synthesizable. The band edge position suggest that $Ti_3O_3N_2$ is particularly interesting as its conduction and valance band bracket the water redox levels and band gap predicted as 2.37 eV, is small enough for visible light absorption (Fig 7). Comparing the band properties of $Ti_3O_3N_2$ with TaON, the best oxynitride photocatalyst so far, it is found that both of them have their Conduction and Valance Band associating the water redox levels, but the band gap of $Ti_3O_3N_2$ is expected to be smaller than the band gap of TaON (2.83 eV in calculation and 2.4 eV in experiment). Therefore, $Ti_3O_3N_2$ has a potential to exhibit better photocatalytic performance than TaON [11].

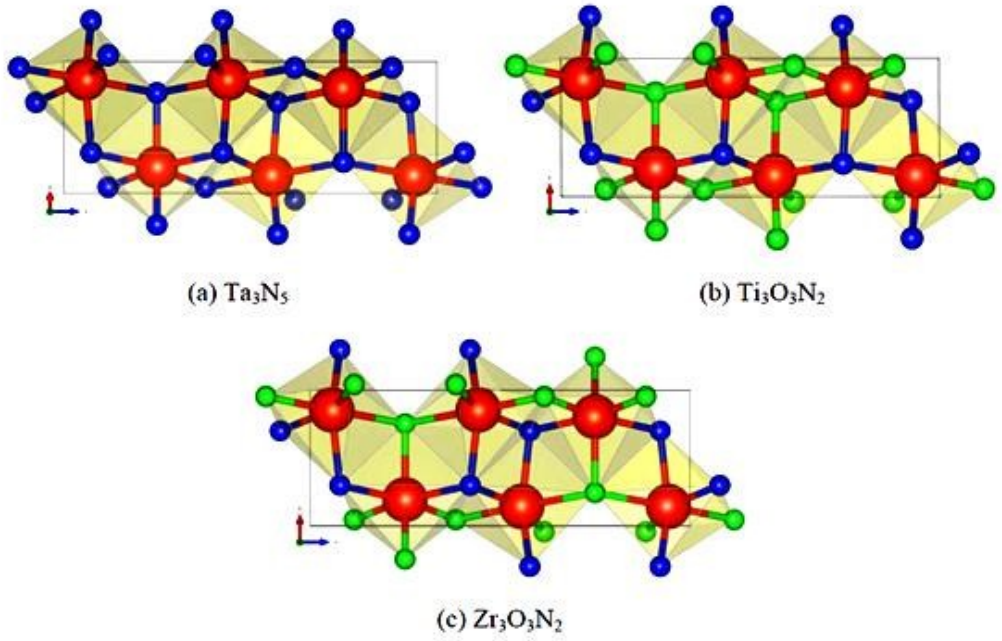

Figure 6: Comparison of crystal structure. Blue atoms are N, green atoms are O and red atoms are (a) Ta, (b) Ti, and (c) Zr (reproduced from ref. 11 with permission from the Royal Society of Chemistry).

$Zr_3O_3N_2$ also has its conduction and valance Band associated with water redox level but it is predicted that band gap of $Zr_3O_3N_2$ is large (3.40 eV). However, Fig.7 suggests that the large band gap of $Zr_3O_3N_2$ is mainly due to its wide conduction band (CB) level and predicted to be a good photocatalysts under UV irradiation without the presence of metal co-catalyst because the conduction band (CB) has sufficient potential for H_2 formation by reduction of water [E_0 (H_2O/H_2) = 0 eV at pH 0] and may also be visible light driven with some CB engineering [61]. Shifting the CB downwards is a relatively easy which can be achieved with cation doping. If its CB can be shifted to be slightly higher than the H_2/H_2O level while retaining its valance band position, the band gap will be reduced to 2.0 eV, making it a promising candidate for visible light driven photocatalysts [11].

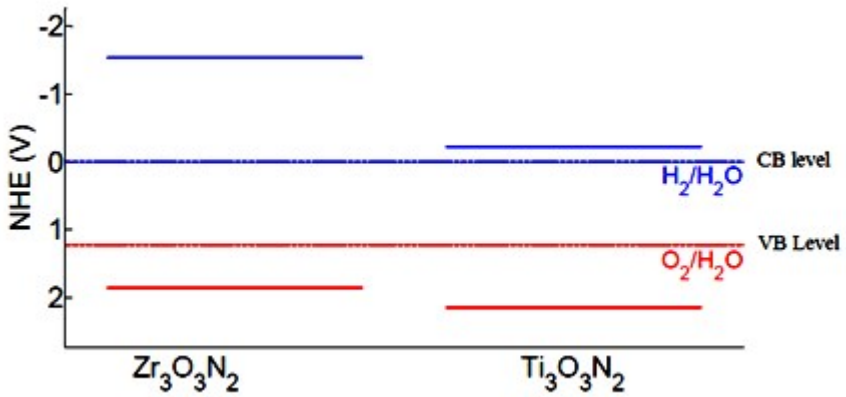

Figure 7: Band gap level of $Zr_3O_3N_2$ and $Ti_3O_3N_2$ with normal hydrogen electrode reference (reproduced from the ref. 11 with permission from the Royal Society of Chemistry).

4.5. Perovskite oxynitrides

Perovskite-type materials are known for numerous kinds of applications because their crystal structure is very flexible towards substitutions since it is possible to control the properties of these materials by suitably modifying their composition [62], which may induce interesting physical properties such as colossal magneto-resistance, superconductivity, photocatalysis activity and visible light photo absorption [63]. Oxynitride perovskite with general formula $ABO_{2-x}N_{1+x}$ were first reported by R. Marchand and co-workers and further investigated by several groups [64]. Oxynitrides perovskite are generally derived from the corresponding oxides by introducing nitrogen into the anionic network. The resulting increase of negative charge is compensated by (i) cationic substitution at the A site (ii) changes in the oxidation state of the transition metal and (iii) reduction of the number of anions [62]. Most substitutions concern the A-site and the transition metals in the B-site of the perovskite lattice, but substitution of the oxygen sites with nitrogen content up to a maximum of 2.16 atoms per formula offers a powerful way to alter the electronic structure of the valence band [65]. The conventional method for the synthesis of oxynitrides is ammonolysis. Synthesis of perovskite type compound (ABO_2N) is generally performed by reactions in NH_3 (g) between 600 °C and 1100 °C, starting with their oxide precursors ($A_2B_2O_7$) or mixtures of oxides and oxysalts e.g. carbonates. The synthesis of the precursors was carried out by either soft-chemistry methods or conventional solid–solid reactions [66]. The use of precursors is needed for rare earths due to the reactivity of R_2O_3 (R = La, lanthanide) in NH_3 is fairly low. However binary rare-earth oxides R_2O_3 usually do not react with transition metal oxides in NH_3 at moderate temperatures so that the ammonolytic synthesis of rare-earth transition-metal oxynitrides requires the use of ternary oxides or very reactive, amorphous precursors. Other convenient methods are solid state reactions in N_2 at higher temperatures (ca. 1500 °C), starting with mixtures of oxynitrides and oxides. High pressure also stabilizes structures with high coordination numbers such as perovskite. However, very few direct solid-state syntheses of oxynitrides at high pressures have been reported [67].

$$A_2B_2O_7 + 2NH_3 \rightarrow 2ABO_2N + 3H_2O$$

Photocatalytic oxynitride-perovskites are a comparatively new research topic. The first report on the photocatalytic water splitting into H_2 and O_2 with an oxynitride photocatalyst

appeared in 2002. Kasahara et al., stated on the photocatalytic properties of $LaTiO_2N$ and $La_{0.75}Ca_{0.25}TiO_{2.75}N_{0.25}$ prepared by thermal ammonolysis of the citric route produced corresponding oxide precursors. $LaTaON_2$ has a perovskite structure with La^{3+} and Ta^{5+} at the A- and B-sites, respectively (Fig. 8) [68]. The tantalum, niobium and titanium oxynitride perovskite are promising candidates for the photocatalytic splitting of water under illumination with visible light. The band gaps and band edge position of $CaTaO_2N$, $SrTaO_2N$, $LaTaON_2$ and $BaNbO_2N$ are suitable for both water oxidation and reduction. They have smaller band gaps than TiO_2 (1.5−2.5 eV) and are stable in aqueous solutions, and the presence of tantalum offers the promise of high efficiency because many of the highest quantum efficiency photocatalyst contain tantalum [69]. For efficient conversion of solar energy, band gaps smaller than 2 eV (equivalent to an absorption edge of 620 nm) are convenient, and the band gaps of this group of compounds range from 1.8 eV (for $LaTaON_2$) to 2.5 eV (for $CaTaO_2N$). The tantalum perovskites is unable to perform overall water splitting. The $LaTaON_2$ evolve H_2 from water (620 nm) but they are not active in O_2 production and show efficiencies in water reduction up to 20 percent [70].

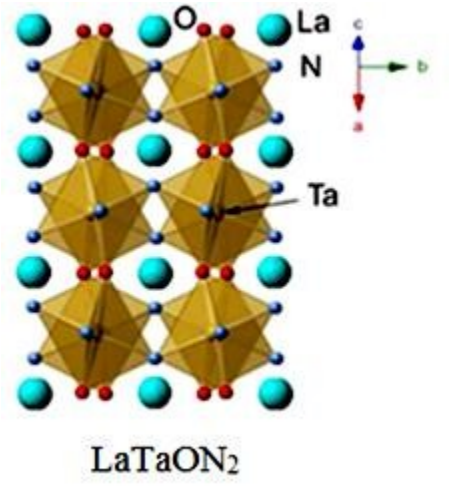

Figure 8: $LaTaON_2$ perovskite structure (reproduced from ref. 71 Open Access Source).

However overall water splitting with visible light up to 600 nm has been recently reported for the double tantalum/magnesium perovskite with formula $LaMg_xTa_{1-x}O_{1+3x}N_{2-3x}$ ($x > 1/3$) can be synthesized by thermal ammonolysis of the corresponding oxides and/or were synthesized by the controlled mixing of (1-3/2x) $LaTaON_2$ and 3/2x $LaMg_{2/3}Ta_{1/3}O_3$ (Fig. 9) [71, 72]. The oxide precursors are prepared via a molecular route called the citric acid method. This method produces an oxide precursor wherein each component can be intimately mixed, and this precursor is suitable for the production of multicomponent crystalline oxynitrides [73].

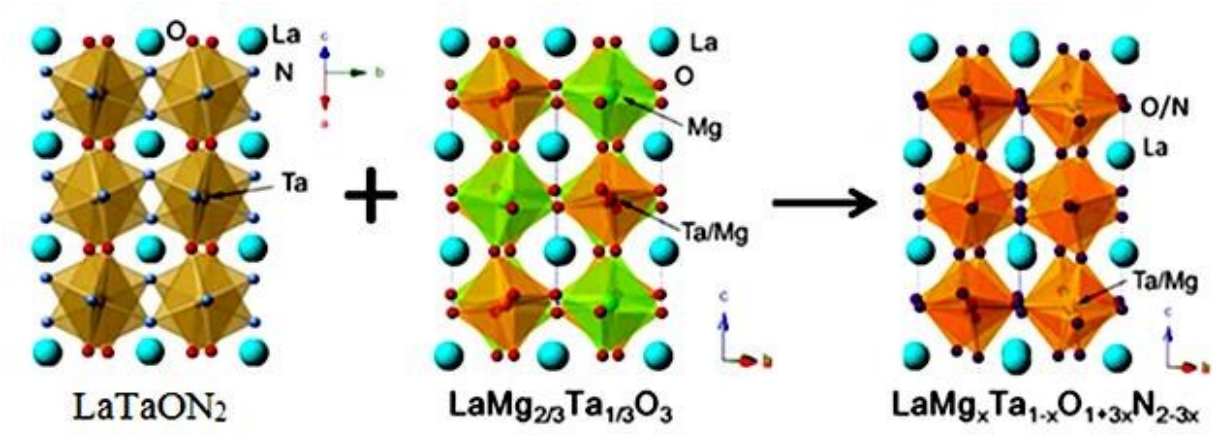

Figure 9: Synthesis and crystal structure of $LaMg_xTa_{1-x}O_{1+3x}N_{2-3x}$ (reproduced from the ref. 72 Open Access).

The similar lattice constants of the precursors enabled the formation of uniform solid solutions with tunable band structures. UV/Vis diffuse reflectance spectra show that the wavelength of the absorption edge of $LaMg_xTa_{1-x}O_{1+3x}N_{2-3x}$ is blue-shifted from 640 to 525 nm when the molar ratio of Mg^{2+} in the solid solution is increased from x=0 to 0.6 (Fig. 10) [71, 72]. The increase in band-gap energy was mainly attributed to the shift in the level of the valence band maximum as a result of the change in O and N content and should be at least advantageous for O_2 evolution. For these oxynitride solid solutions, the lower part of the conduction band mainly consists of Ta_{5d} orbitals, while the upper part of the valence band consists mainly of N_{2p} orbitals with a small contribution from O_{2p} orbitals. The increase in Mg content decreases the N/O ratio, which shifts the VBM downward [74]. The concept for the band engineering by compositional tuning is schematically illustrated in Fig. 11. The $LaMg_{1/3}Ta_{2/3}O_2N$ solid solution (x=1/3) with a band-gap energy of 2.08 eV was identified as the most suitable one for overall water splitting [75].

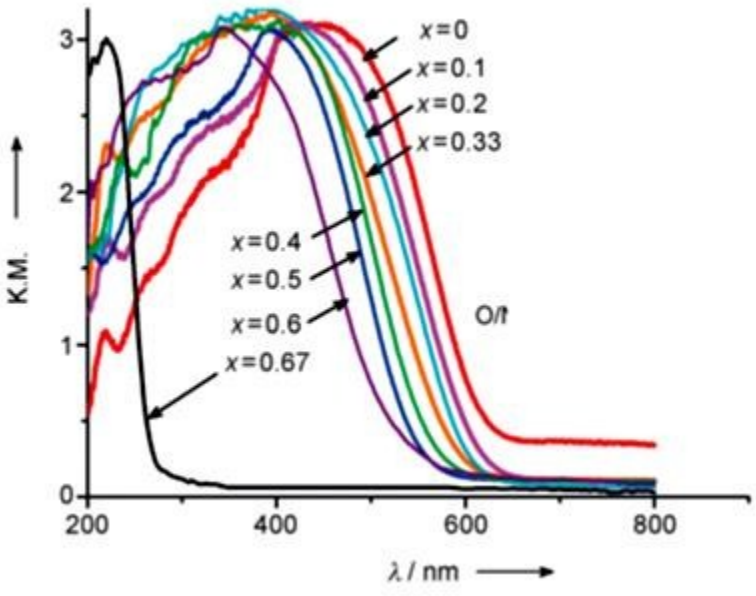

Figure 10: UV/Vis diffuse reflectance spectra of the $LaMg_xTa_{1-x}O_{1+3x}N_{2-3x}$ photocatalyst (reproduced from ref. 72 Open Access).

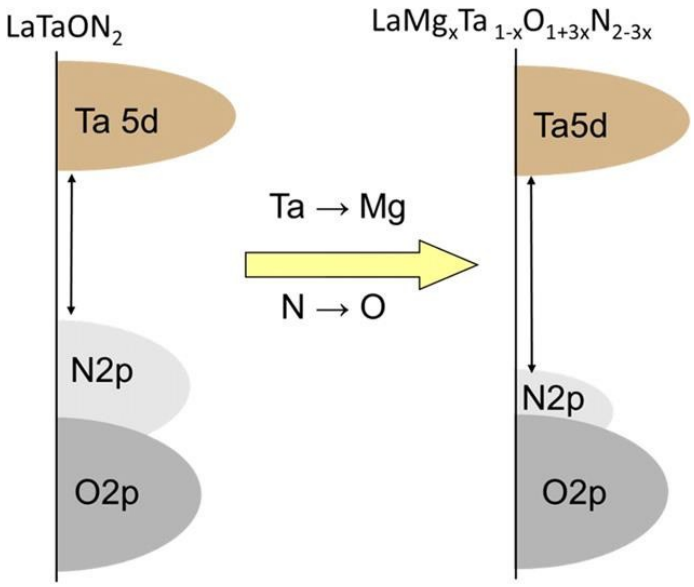

Figure 11: Schematic of band engineering by compositional tuning (reproduced from the ref. 72 Open Access).

Zhang et al. reported n-type semiconductor $LaTiO_2N$ oxynitride (LTON) material with a perovskite structure and a band gap of 2.1 eV (~600 nm absorption edge). LTON is favorable for water splitting due to low energy band positions and also prepared by relatively cheap material. In the previous work Kasahara et al. found that using this material, water splitting for H_2 and O_2 production in the presence of sacrificial reagent is theoretically and experimentally feasible under visible light irradiation. Although a quantum efficiency of ~5% for water oxidation has been achieved using IrO_2-loaded LTON. The quantum efficacy can be further improved if precious co-catalyst IrO_2-loaded LTON replaced with a more earth abundant metal species.

$LaTiO_2N$ CoO_x-modified photocatalyst synthesized by flux (FX) and polymerized complex (PC) method using oxide precursors ($La_2Ti_2O_7$) under a flow of NH_3 at 1223 K. The obtained nitride powders are referred to as FX-LTON and PC-LTON, respectively. Cobalt oxide (CoO_x) was deposited on $LaTiO_2N$ samples as a co-catalyst by an impregnation method from aqueous $Co(NO_3)_2$ solution, followed by NH_3 treatment at 973 K and calcination at 473 K in air.

CoO_x co-catalyst was most efficient as compare to IrO_2 which is well known as one of the most efficient water oxidation co-catalyst and also resulted in marked enhancement in the water oxidation activity. The optimize CoO_x-LTON was found high efficiency of 27.1 ± 2.6% at 440 nm which significantly exceeds the value reported for pervious particulate photo-catalyst with a 600 nm absorption edge. Further they notice that FX-LTON gave a higher performance than PC-LTON. The significantly enhanced quantum efficiency can be attributed to improvements in both the photocatalyst and co-catalyst component [68, 76].

4.5.1. Niobium Based Perovskite Oxynitrides:

Hisatomi et al reported that Niobium-based perovskite type oxynitrides, $ANb(O,N)_3$ (A= Ca, Sr, Ba, and La) are potential candidates for a water splitting photocatalyst with a wide visible light absorption band. They have smaller band gap energies than the corresponding Ta-based analogues oxynitrides because the conduction band of Nb formed by the empty Nb_{4d} orbitals lies at a more positive potential than the Ta_{5d} and of the higher electronegativity of Nb. $BaNbO_2N$ is of particular interest for solar energy conversion because it was found to be inactive for both oxygen and hydrogen evolution reaction and of its narrow band gap of 1.7 eV allowing light absorption up to 740 nm.

$BaNbO_2N$ was synthesized by nitriding the corresponding oxide precursor $Ba_5Nb_4O_{15}$ under an NH_3 flow. The oxide precursor, $Ba_5Nb_4O_{15}$ was prepared by calcining a mixture of $BaCO_3$ and Nb_2O_5, with NaCl added as a flux at 1173 K. After a slow cool-down to room temperature, the oxide sample was rinsed with copious amounts of distilled water to eliminate the NaCl flux. $BaCO_3$ was added to $Ba_5Nb_4O_{15}$ before nitridation to suppress the possible generation of niobium oxynitride.

Each of the niobium compounds is found to be iso-structural with its tantalum analogue. Interestingly, the niobium compounds consistently have a unit cell volume that is larger than its tantalum analogue by 0.7-1.2%. In the diffuse reflectance spectra (DRS) of the nitridation products, the onset of light absorption characteristics of the band gap excitation of $BaNbO_2N$ was observed at around 740 nm (Fig. 12). Additional light absorption was observed in the longer wavelength region, which could be attributed to defects such as reduced B-site cations (Nb) and anion vacancies. Hisatomi et al. also demonstrated that that $BaNbO_2N$ can be activated for photocatalytic water splitting in the presence of sacrificial reagents by modifying the starting material for nitridation and loading appropriate co-catalysts. $BaNbO_2N$ generates oxygen from

an aqueous $AgNO_3$ solution under illumination up to 740 nm, the longest wavelength ever reported for (oxy) nitride photocatalysts [77-79].

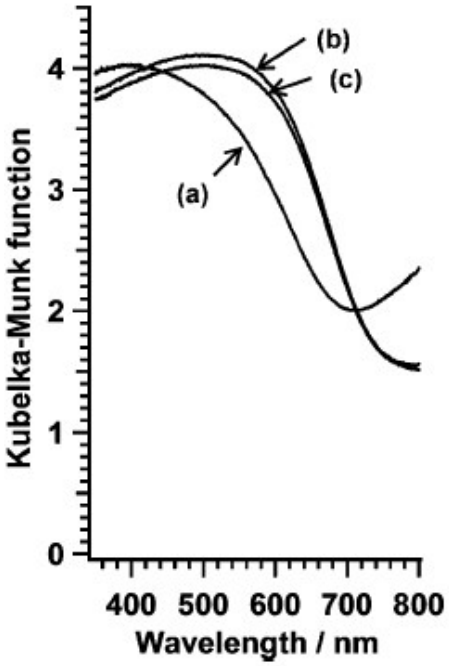

Figure 12: Diffuse reflectance spectra of $BaNbO_2N$ oxynitride, nitride from $BaCO_3$ and Nb_2O_5 a) 100 b) 300 and c) 500 $mLmin^{-1}$ NH_3 (reproduced from the ref. 76 with permission from the Royal Society of Chemistry).

5. EFFECT OF ELECTROLYTE ON ACTIVITY OF PHOTOCATALYSIS

Most of the research in photocatalytic water splitting has been reported are materials based and has been extensively studied as a potential method to supply hydrogen from sunlight and water. Only few have investigated the effects of the electrolytic environment on photocatalytic efficiency [81-83]. Many researcher investigated photocatalyst water splitting using a variety of electrolyte including H_2SO_4, KNO_3, NaCl, and Sodium acetate, H_3PO_4, $NaClO_4$ and KOH [84-88]. However, there has been a slight comparison between different electrolytes on photocatalytic activity. From the prospective of particle application, the ability to produce hydrogen from the natural seawater would be highly desirable as seawater is most abundant water resource in the world. However, seawater (act as an electrolyte) contains numbers of inorganic anions and cations and effect of such ions on the activity of water splitting reaction remains to be investigated in more detail. The effect of electrolyte (identity and concentration) in overall water splitting reaction have to rigorously and quantitatively taken into account because they may

cause reaction switching and additional adsorption onto the active sites, which may enhance or decreases the overall catalytic efficiency. Some studies reported that electrolyte reduces the efficiency of photocatalyst but some reported improved effect and some researcher found that electrolytes at high pH are more effective in promoting photocatalytic water splitting [89, 90].

Ji and co-worker investigated the overall water splitting in seawater using NiO_x-Loaded $La_2Ti_2O_7$ under ultraviolet irradiation (λ>200 nm). They reported that water splitting can be achieved in seawater, although at half the rate of activity as compared to that in pure water. It was concluded that the suppression of activity in seawater is mainly due to the presence of magnesium cation in the reactant solution. Their study also investigated the visible light photocatalytic activity of a platinum loaded CdS/TiO_2 composite catalyst for hydrogen production in the presence of SO_3^{2-} and S^{2-} as sacrificial electron donor and a Fe_2O_3 thin-film electrode for anodic photo-current generation [91].

Medea et al. investigated the effects of various electrolytes on the photocatalytic activity of $(Ga_{1-x}Zn_x)$ $(N_{1-x}O_x)$ for overall water splitting under visible light irradiation (λ>400 nm) with respect to the physicochemical properties of $(Ga_{1-x}Zn_x)$ $(N_{1-x}O_x)$, the co-catalyst and the pH of the reactant solution. The highest activity for overall water splitting achieved by this photocatalytic system, has been obtained using $(Ga_{1-x}Zn_x)$ $(N_{1-x}O_x)$ modified $Rh_{2-y}Cr_yO_3$-loaded co-catalyst in aqueous H_2SO_4 solution at pH 4.5. They also notice that addition of an appropriate amount of electrolyte such as NaCl and Na_2SO_4 to the reactant solution enhance overall water splitting reaction. Addition of electrolytes, particularly NaCl and Na_2SO_4, to the reactant solution might facilitate surface redox reactions and/or compensate for the detrimental effect of surface defects that can act as recombination centers between photogenerated electrons and holes, thereby enhancing activity [92]. However the same photocatalyst was also demonstrated to split artificial seawater under visible light irradiation, approximately half of the activity achieved as compare to the pure water. Similar positive effects on photocatalytic activity for overall water splitting by electrolyte addition have been observed for UV active metal-oxide photocatalysts, although the mechanism for such an effect has not been reported [93].

6. CONCLUSION

Photocatalyst are expected to be a future trend, since nano-sized photocatalysts have shown much better performance than their bulk counterparts. In literature a lot of research is reported over the past few decades, in which an attempt is made to develop a photocatalyst with the

highest activity. Development of a large number of photocatalysts and screen them for their activity is the general applied method but more fundamental approach is to improved simple screening. In general, light absorption, electron-hole separation, hole transportation, and surface reaction are the key features in research and design, requiring materials of optimized composition, favorable structure, and morphology. Therefore i tried to give more insight into the subject of photocatalysis for future.

The first step in syntheses of a suitable photocatalyst is to tune the band gap in such a way that it should lies between 1.6 and < 3 eV. The valence band should be lower in energy than the oxidation potential of oxygen and subsequently the conduction band should be higher than the reduction potential of hydrogen. Because the reaction proceeds via half reactions using ions, it is preferable that the photocatalyst splits water heterolytically into a proton and a hydroxyl anion and must reduce generation of water from molecular oxygen and hydrogen. This can be facilitated by use of suitable metal oxides precursor. Most of photocatalyst are limited for half reaction so a co-catalyst is necessary to create hydrogen gas. In addition the design photocatalyst must perform the same properties as like semiconductor.

Recently there has been significant progress in the development of metal oxynitrides and have been studies a potential visible-light photocatalyst with appreciable activities. This development has laid a good foundation for future work in this area. The improvement of new technologies needs collaboration with a strong theoretical background for a better understanding of the hydrogen production mechanism, in order to come up with a low-cost and environmentally friendly water-splitting process for hydrogen production.

REFERENCES

1. B. Adeli and F. Taghipour, *ECS J. Solid State Sci. Technol.,* 2013, **2,** 118-126

2. F.E. Osterloh and B.A. Parkinson, *MRS Bull.,* 2011, **36**, 17-22

3. R.M.N. Yerga, M.C.A. Galvan, F. del Valle, J.A.V. de la Mano and J.L.G. Fierro, *ChemSusChem,* 2009, **2**, 471- 485

4. P. Kanhere and Z. Chen, *Molecules,* 2014, **19**, 19995-20022

5. J. Zhu and M. Zach, *Curr. Opin. Colloid Interface Sci.* 2009, **14**, 260-269

6. B. Cao, G. M, Veith, R. E. Diaz, J. Liu, E. A. Stach, R. R. Adzic and P. G. Khalifah, *Angew. Chem.,* 2013, **125**, 10953-10957

7. M. Yang, J. Ore-Sole, J. A. Rodgers, A. B. Jorge, A. Fuertes and J. P. Attifield, *Nature Chem.*, 2011, **3**, 47-52

8. F. E. Osterloh, *Chem. Mater.*, 2008, **20**, 35-54

9. K. Maeda and K. Domen, *J. Phys. Chem.*, 2007, **111**, 7851-7861

10. S.M. Ji, P.H. Borse, H.G. Kim, D.W. Hwang, J.S. Jang, S.W. Bae and J.S. Lee, *Phys. Chem. Chem. Phys.*, 2005, **7**, 1315-1321

11. Y. Wu, P. Lazic, G. Hautier, K. Persson and G. Ceder, *Energy & Environ. Sci.*, 2013, **6**, 157-168

12. A. Fuertes, *Dalton Trans.*, 2010, **39**, 5942-5948

13. D. Logvinovich, Doctoral Dissertation, Solid State Chemistry and Catalysis. 2008

14. Z. F. Huang, L. Pan, J. J. Zou, X. Zhang and L. Wang, *Nanoscale*, 2014, **6**, 14044-14063

15. L. Yang, H. Zhou, T. Fan, and D. Zhanga, *Phys. Chem. Chem. Phys.*, 2014, **16**, 6810-6826

16. J. Zhu and M. Zäch, *Curr. Opin. Colloid Interface Sci.*, 2009, **14**, 260-269

17. A.B. Murphy, P.R.F. Barnesa, L.K. Randeniyaa, I.C. Plumba, I.E. Greyb, M.D. Horneb and J.A. Glasscocka, *Int. J. Hydrogen Energy*, 2006, **31,** 1999 -2017

18. Y. Sakata, Y. Matsuda, T. Yanagida, K. Hirata, H. Imamura and K. Teramura, *Catalysis Lett.*, 2008, **125**, 22-26

19. T. Kurushima, G. Gundiah, Y. Shimomura, M. Mikami, N. Kijima and A. K. Cheetham, *J. Electrochem. Soc.*, 2010, **157**, 64-68.

20. R. Marchanda, Y. Laurenta, J. Guyadera, P. L'Haridona and P. Verdiera, *J. Eur. Ceram. Soc.*, 1991, **8**, 197-213.

21. S. H. Elder, F. J. Di Salvo, L. Topor, A. Navrotsky. *Chem. Mater*., 1993, **5**, 1545-1553.

22. G. Tessier and R. Marchand, *J. Solid State Chem*., 2000, **171**, 143-151.

23 M. R. Brophy, S. M. Pilgrim and W. A. Schulze, *J. Am. Ceram. Soc.*, 2011, **94**, 4263-4268.

24. A. Hellwig and A. Hendry, *J. Mater. Sci*., 1994, **29**, 4686-4693

25. S. J. Clarke, B. P. Guinot, C. W. Michie, M. J. C. Calmont and M. J. Rosseinsky, *Chem. Mater.*, 2002, **14**, 288-294.

26. Y. Kim, W. Si, P. M. Woodward, E. Sutter, S. Park and Y. Vogt, *Chem. Mater.*, 2007, **19**, 618-623

27. C. Le Paven-Thivet, A. Ishikawa, A. Ziani, L. Le Gendre, M. Yoshida, J. Kubota, F. Tessier and K. Domen, *J. Phys. Chem. C.*, 2009, **113**, 6156-6162.

28. E. Martınez-Ferrero, Y. Sakatani, C. Boissiere, D. Grosso, A. Fuertes, J. Fraxedas and C. Sanchez, *Adv. Funct. Mater*, 2007, **17**, 3348-3354

29. A. Fujishima and K. Honda, *Nature*, 1972, **238**, 37-38

30. Y. Moriya, T. Takata, K. Domen, *Coord. Chem. Rev.*, 2013, **257**, 1957-1969.

31. M. Pelaez, et al (2012). *Appl. Catal. B: Environ.*, 2012, **125**, 331-349.

32. J. Kubota and K. Domen, *The Electrochem. Soc. Interface,* 2013, **22**, 57-62.

33. K. Maeda, K. Teramura, D. Lu, T. Takata, N. Saito, Y. Inoue and K. Domen, *Nature*, 2006, **440**, 295

34. K. Maeda, H. Hashiguchi, H. Masuda, R. Abe and K. Domen, *J. Phys. Chem. C.*, 2008, **112**, 3447-3452.

35. C. M. Fang, E. Orhan, G. A. De Wijs, H. T. Hintzen, R. A. De Groot, R. Marchand, J. Y. Saillard and G. De With, *J. Mater. Chem.*, 2001, **11**, 1248-1252

36. M. Yashima, Y. Lee and K. Domen, Activity Report on Neutron Scattering Research: *Experimental Reports*, 15, 2008

37. M. Hara, E. Chiba, A. Ishikawa, T. Takata, J. N. Kondo and K. J. Domen, *Phys. Chem., B.*, 2003, **107**, 13441-13445.

38. G. Hitoki, A. Ishikawa, T. Takata, J. N. Kondo, M. Hara and K. Domen, *Chem. Lett.*, 2002, **31**, 736-737.

39. A. Ishikawa, T. Takata, J. N. Kondo, M. Hara and K. Domen, *J. Phys. Chem. B.*, 2004, **108**, 11049-11053.

40. K. Ueda, H. Kato, M. Kobayashi, M. Hara and M. Kakihana, *J. Mater. Chem. A.*, 2013, **1**, 3667-3674.

41. P. Li, W. Fan, Y. Li, H. Sun, X. Cheng, X. Zhao and M. Jiang, *Inorg. Chem.*, 2010, **49**, 6917-6924.

42. D. Armytage and B.E.F. Fender, *Acta Crystallogr., Sect. B: Struct. Crystallogr. Cryst. Chem.*, 1974, **30**, 809-812

43. K. Maeda, D. Lu and K. Domen, *Angew. Chem. Int. Ed.*, 2013, **52**, 6488-6491.

44. R. Nakamura, T. Tanaka, Y. Nakato, *J. Phys. Chem. B.*, 2005, **109**, 8920-8927

45. A. Fuertes, *Materials Horizons*, 2015, **2**, 453-461

46. H.N. Kim, "Photocatalytic Water Splitting Reactions Based on Tantalum Oxynitrides" *Literature Seminar*, October 15, 2013

47. F.A., Ponce and D. P. Bour, *Nature*, 1997, **386**, 351-359.

48. I. M. Huygens, K. Strubbe and W. P. Gomes, *J. Electrochem. Soc.*, 2000, **147**, 1797-1802.

49. M. J. Chen, J. R. Yang and M. Shiojiri, *Semicond. Sci. Technol.*, 2012, **27**, 074005.

50. Y. S. Choi, J.W. Kang, D. K. Hwang and S. J. Park, *IEEE T. Electron. Dev.*, 2010, **57**, 26-41

51. S.P. Phivilay, C. A. Roberts, A.A. Puretzky, K. Domen, and I. E. Wachs, *J. Phys. Chem. Lett.*, 2013, **4**, 3719-3724.

52. Y. Lee, H. Terashima, Y. Shimodaira, K. Teramura, M. Hara, H. Kobayashi, K. Domen and M. Yashima, *J. Phys. Chem. C.*, 2007, **111**, 1042-1048.

53. K. Maeda, K. Teramura, D. Lu, N. Saito, Y. Inoue and K. Domen, *J. Phys. Chem. C.*, 2007, **111**, 7554-7560.

54. K. Maeda, T. Takata, M. Hara, N. Saito, Y. Inoue, H. Kobayashi and K. Domen, *J. Am. Chem. Soc.*, 2005, **127**, 8286-8287.

55. Z. Wang,a Y. Liu, B. Huang, Y. Dai, Z. Lou, G. Wang, X. Zhanga and X. Qina, *Phys.Chem.Chem.Phys.*, 2014, **16**, 2758-2774.

56. G. Hitoki, T. Takata, J. N. Kondo, M. Hara, H. Kobayashi and K. Domen, *Chem. Commun.*, 2002, **16**, 1698-1699.

57. K. Maeda, K. Teramura, N. Saito, Y. Inoue, H. Kobayashi, and K. Domen, *Pure Appl. Chem.*, 2006, **78**, 2267-2276.

58. Z. Zou and H. Arakawa, *J. Photochem. Photobiol. A.* 2003, **158**, 145-150.

59. K. Maeda et al., *J. Phys. Chem. B.* 2005, **109**, 20504-20510.

60. K. Kamata, K. Maeda, D. Lu, Y. Kako , K. Domen, *Chem. Phys. Lett.*, 2009, **470**, 90-94.

61. T. Mishima, M. Matsuda and M. Miyake, *Appl.Catal. A: General*, 2007, **324**, 77-82.

62. A. Rachel, S.G. Ebbinghaus , M. Gungerich, P.J. Klar J. Hanss, A. Weidenkaff and A. Reller *Thermochimica Acta*, 2005, **438,** 134-143.

63. D. Oka , Y. Hirose, H. Kamisaka, T. Fukumura, K. Sasa, S. Ishii, H. Matsuzaki, Y. Sato, Y. Ikuhara and T. Hasegawa, *Sci. Rep.*, 2014, **4,** 4987.

64. R. Marchand, *C.R. Acad. Sci. Paris*, 1976, **282**, 329-348.

65. A. E. Maeglia, E. H. Otala, T. Hisatomib, S. Yoona, C. M. Leroyb, N. Schäublea, Y. Lua, M. Grätzelb and A. Weidenkaff, *Energy Procedia.*, 2012, **22**, 61-66.

66. F. Tessier, R. Marchand, *J. Solid State Chem.*, 2003, **171**, 143-151.

67. M. Yang, J. A. Rodgers, L. C. Middler, J. Oro-Sole, A. B. Jorge, A. Fuertes and J. P. Attfield, *Inorg. Chem.*, 2009, **48**, 11498-11500.

68. A. Kasahara, K. Nukumizu, G. Hitoki, T. Takata, J. N. Kondo, M. Hara, H. Kobayashi and K. Domen, *J. Phys. Chem. A.*, 2002, **106**, 6750-6753.

69. S. Balaz, H. S. Porter, M. P. Woodward and J. L. Brillson, *Chem. Mater.*, 2013, **25**, 3337-3343.

70. D. Yamasita, T. Takata, M. Hara, J. N. Kondo and K. Domen, *Solid State Ionics*, 2004, **172**, 591-595.

71. C. Pan, T. Takata, M. Nakabayashi, T. Matsumoto, N. Shibata, Y. Ikuhara, and K. Domen, *Angew. Chem. Int. Ed.*, 2015, **54**, 2955-2959.

72. T. Takata, C. Pan and K. Domen, *Sci. Technol. Adv. Mater.*, 2015, **16**, 033506 (18pp)

73. C. Marcilly, P. Courty and B. Delmon, *J. Am. Ceram. Soc.*, 1970, **53**, 56-57.

74. Y. I. Kim and P. M. Woodward, *J. Solid State Chem.*, 2007, **180**, 3224-3233.

75. J. Zhang and X. Wang, *Angew. Chem. Int. Ed.*, 2015, **54**, 7230-7232.

76. F. Zhang, A. Yamakata, K. Maeda, Y. Moriya, T. Takata, J. Kubota, K. Teshima, S. Oishi, and K. Domen, *J. Am. Chem. Soc.*, 2012, **134**, 8348-8351.

77. T. Hisatomi, C. Katayama, Y. Moriya, T. Minegishi, M. Katayama, H. Nishiyama, T. Yamadad and K. Domen, *Energy Environ. Sci.*, 2013, **6**, 3595-3599.

78. T. Hisatomi, C. Katayama, K. Teramura, T. Takata, Y. Moriya, T. Minegishi, M. Katayama, H. Nishiyama, T. Yamada, and K. Domen, *ChemSusChem.*, 2014, **7**, 2016-2021.

79. B. Siritanaratkul, K. Maeda, T. Hisatomi, and K. Domen, *ChemSusChem.*, 2011, **4**, 74-78.

80. H. L. Wang, T. Deutsch, J. A. Turner, *J. Electrochem. Soc.*, 2008, **155**, F91-96

81. E. L. Miller, B. Marsen, D. Paluselli, R. Rocheleau, *Electrochem. Solid-State Lett.*, 2005, **8**, A247-249

82. J. Greeley, T. F. Jaramillo, J. Bonde, I. B. Chorkendorff, J. K. Norskov, *Nature Mater.*, 2006, **5**, 909-913

83. E. Bae, W. Choi, *J. Phys. Chem. B*, 2006, **110**, 14792-14799

84. W. B. Ingler, S. U. M. Khan, *Electrochem. Solid-State Lett.*, 2006, **9**, G144-146

85. A. Belghazi, S. Bohm, D. A. Worsley, H. N. McMurray, Z. *Phys. Chem.*, 2005, **219**, 1539-1546

86. T. F. Jaramillo, S. H. Baeck, A. Kleiman-Shwarsctein, K. S. Choi, G. D. Stucky, E. W. McFarland, *J. Comb. Chem.*, 2005, **7**, 264-271

87. Y. F. Su, T. C. Chou, T. R. Ling, C. C. Sun, *J. Electrochem. Soc.*, 2004, **151**, A1375-1382

88. E. Thimsen, N. Rastgar, P. Biswas, *J. Phys. Chem. C.*, 2008, **112**, 4134-4140

89. S. Q. Zhang, H. J. Zhao, D. L. Jiang, R. John, *Anal. Chim. Acta.*, 2004, **514**, 89-97

90. C. B. Almquist, P. Biswas, *Chem. Eng. Sci.*, 2001, **56**, 3421-3430

91. S.M. Ji, H. Jun, J.S. Jang, H.C. Son, P.H. Borse, J.S. Lee, *J. Photochem. Photobiol. A: Chem.*, 2007, 189, 141-144

92. K. Maeda, H. Masuda, K. Domen, *Catal. Today*, 2009, **147**, 173-178

93. K. Sayama, H. Arakawa, *J. Photochem. Photobiol. A: Chem.*, 1996, **94**, 67-76